The FASEB Journal express article 10.1096/fj.03-0402fje. Published online November 20, 2003.

Epicatechin, catechin, and dimeric procyanidins inhibit PMA-induced NF-κB activation at multiple steps in Jurkat T cells

Gerardo G. Mackenzie,* Fernando Carrasquedo,[†] José M. Delfino,* Carl L. Keen,[†,‡] César G. Fraga,[§] and Patricia I. Oteiza*[,†,¶]

*Departamento de Química Biológica, Instituto de Química y Fisicoquímica Biológicas; [§]Fisicoquímica, Programa de Radicales Libres, (Universidad de Buenos Aires, Consejo Nacional de Investigaciones Científicas y Técnicas), Facultad de Farmacia y Bioquímica, Universidad de Buenos Aires; and Departments of [†]Nutrition, [¶]Environmental Toxicology, and [‡]Internal Medicine, University of California–Davis

Corresponding author: Patricia I. Oteiza, Department of Nutrition, University of California, Davis, California, 95616. E-mail: poteiza@ucdavis.edu

ABSTRACT

The capacity of the flavan-3-ols [(–)-epicatechin (EC) and (+)-catechin (CT)] and a B dimeric procyanidin (DP-B) to modulate phorbol 12-myristate 13-acetate (PMA)-induced NF-κB activation in Jurkat T cells was investigated. The classic PMA-triggered increase in cell oxidants was prevented when cells were preincubated for 24 h with EC, CT, or DP-B (1.7–17.2 μM). PMA induced the phosphorylation of IKKβ and the subsequent degradation of IκBα: These events were inhibited in cells pretreated with the flavonoids. PMA induced a 4.6-fold increase in NF-κB nuclear binding activity in control cells. Pretreatment with EC, CT, or DP-B decreased PMA-induced NF-κB binding activity and the transactivation of the NF-κB-driven gene IL-2. EC, CT, and DP-B inhibited, in vitro, NF-κB binding to its DNA consensus sequence, but they had no effect on the binding activity of CREB or OCT-1. Thus, EC, CT, or DP-B can influence the immune response by modulating NF-κB activation. This modulation can occur at early (regulation of oxidant levels, IKK activation) as well as late (binding of NF-κB to DNA) stages of the NF-κB activation cascade. A model is presented for possible interactions between DP-B and NF-κB proteins, which could lead to the inhibition of NF-κB binding to κB sites.

Key words: (–)-epicatechin • (+)-catechin • dimeric procyanidin • immune response • IL-2

Flavonoids are natural substances present in cocoa and wine as well as apples, grapes, tea, and other plants and are thought to have beneficial effects on human health (1–4). Such beneficial effects are due in part to their antioxidant and anti-inflammatory properties, which could lead to diminished vascular and platelet reactivity (5–7).

Chemically, flavan-3-ols constitute a subgroup of flavonoids that includes (–)-epicatechin (EC) and (+)-catechin (CT). The oligomers synthesized upon EC and CT are called procyanidins, which in cocoa, are mostly formed by B-bonds between EC (8, 9). Flavan-3-ols and B-

procyanidins have been shown to have the ability to scavenge free radicals, reduce the rate of LDL oxidation, inhibit lipid peroxidation, and participate in the modulation of the immune response in several biological systems (10–14).

Rel/NF-κB transcription factors, which can be activated by multiple signals, regulate the expression of numerous genes that can in turn modulate the immune response (15, 16). The Rel/NF-κB family of proteins in eukaryotic cells includes c-Rel, RelB, RelA (p65), p50/p105, and p52/p100. Rel/NF-κB homo- and heterodimers are commonly in inactive forms in the cytoplasm due to their interaction with inhibitory IκB proteins (17). In general, the phosphorylation of two serines (S32 and S36) present in IκB mediates the activation of NF-κB by specific IκB kinases (IKK) (18). IKK is a large complex composed of a regulatory subunit, IKKγ, and two catalytic subunits, IKKα and IKKβ (19). Once IκBα is phosphorylated, ubiquitination and subsequent degradation are needed for the complete activation of NF-κB (20). The active dimer then translocates to the nuclei in a process partially regulated by the cytoskeleton (21, 22). In the nuclei, NF-κB modulates the transcription of numerous genes involved in the immune and stress response, as well as in the apoptosis of certain cells (15).

In T-cells, NF-κB transcription factor regulates a series of genes that are required for immune responses, including IL-2, IL-6, IL-8, IL-1β, and T-cell surface receptors (16, 23–25). A series of papers have demonstrated that in certain cell types, procyanidins can modulate the expression of IL-2, IL-1β, and IL-4 (23–26). We hypothesized that the flavan-3-ol monomers, EC and CT, and B-type dimeric procyanidins oligomers of the above (DP-B), which can be measured in plasma after the consumption of flavonoid-rich foods (8), could affect the immune response by modulating NF-κB. The objective of this work was to investigate the possible modulation of PMA-induced NF-κB activation by flavan-3-ol monomers and dimers, and to characterize the step(s) in the activation cascade at which they act.

MATERIALS AND METHODS

Materials

EC, CT, and DP-B isolated from Cocoapro cocoa were purified (8, 9) and supplied by Mars Inc. (Hackettstown, NJ). Jurkat (T cell leukemia, human) cells were obtained from the American Type Culture Collection (Manassis, VA). Cell culture media and reagents were obtained from Invitrogen Life Technologies (Carlsbad, CA). The oligonucleotides containing the consensus sequence for NF-κB, OCT-1, CREB, and the reagents for the EMSA assay were obtained from Promega (Madison, WI). The human-IL-2 ELISA assay and the protease inhibitor cocktail were obtained from Roche Applied Sciences (Mannheim, Germany). Antibodies for RelA, p50, and IκBα were obtained from Santa Cruz Biotechnology (Santa Cruz, CA). Phospho-IκBα (p-IκBα) and phospho-IKKβ (p-IKKβ) antibodies were obtained from Cell Signaling Technology (Beverly, MA). PVDF membranes were obtained from Bio-Rad (Hercules, CA), and Chroma Spin-10 columns were obtained from Clontech (Palo Alto, CA). The ECL Western blotting system was obtained from Amersham Pharmacia Biotechnology (Piscataway, NJ). Propidium iodide and 5 (or 6)-carboxy-2'7'-dichlorodihydrofluorescein diacetate (DCDCDHF) probes were obtained from Molecular Probes (Eugene, OR). All other reagents were the highest quality available and were purchased from Sigma (St. Louis, MO).

Cell culture and incubations

Jurkat T cells were cultured in RPMI 1640 media supplemented with 10% fetal bovine serum (FBS) and an antibiotic and antimicotic (10 U/ml penicillin and 10 μg/ml streptomycin, respectively). Cells (1×10^6 cells/ml) were preincubated with 1.7–17.2 μM EC, CT, and DP-B for 24 h. The number of viable cells was measured by exclusion of the dye Trypan Blue. The exposure of cells to different concentrations of EC, CT, or DP-B for 24 h did not affect the number of viable cells (data not shown). Cells were subsequently incubated without or with 100 ng/ml PMA and harvested at 2.5–240 min after incubation.

Determination of cell EC, CT, and DP-B concentrations

After 24 h incubation with 1.7–17.2 μM EC, CT, or DP-B, cells (1×10^7) were collected by centrifugation at 800*g* for 10 min and washed once with phosphate-buffered saline (PBS) containing a 100-fold excess of CT (cells incubated in the presence of EC or DP-B) or EC (cells incubated in the presence of CT) and then washed twice with cold PBS. Total cell fractions were prepared as described below. For the isolation of the nuclei, the cell pellet was resuspended in 4 ml ice-cold 10 mM Tris-HCl buffer, pH 8.0, containing 0.32 M sucrose, 3 mM $CaCl_2$, 2 mM $MgCl_2$, 0.1 mM EDTA, 1 mM DTT, and 0.5% (v/v) Igepal. Cells were homogenized with a manual homogenizer. The suspension was added with 4 ml ice-cold 10 mM Tris-HCl buffer, pH 8.0, containing 2 M sucrose, 5 mM $MgCl_2$, 0.1 mM EDTA, and 1 mM DTT, mixed and layered onto 4 ml of the same buffer. After 45 min of centrifugation at 30,000*g* in a swinging bucket rotor at 4°C, the supernatant fraction was removed and the nuclear pellet was resuspended in 50 mM Tris-HCl buffer, pH 7.5, containing 0.25 M sucrose, 25 mM KCl, and 5 mM $MgCl_2$. The presence of intact nuclei in this fraction was verified by fluorescence microscopy of 4',6'-diamino-2-phenylindole, dihydrochloride-stained fractions (data not shown).

EC, CT, and DP-B were determined by HPLC (HP 1100 HPLC system) with a coularray detector (27, 28). To evaluate the DNA content, samples were added with 50 μM propidium iodide. After incubating for 20 min at room temperature, the fluorescence (λ_{exc}: 538, λ_{em}: 590) was measured.

Electrophoretic mobility shift assay (EMSA)

Nuclear fractions were isolated as described previously (29, 30). At the corresponding time points, cells were collected by centrifugation at 800*g* for 10 min, the pellet (6×10^6 cells) was resuspended in 200 μl of buffer A (10 mM HEPES, pH 7.9, 1.5 mM $MgCl_2$, 10 mM KCl, 0.5 mM DTT, 0.1% Igepal), incubated for 10 min at 4°C, and centrifuged for 1 min at 12,000*g*. The supernatant fraction was discarded, and the nuclear pellets were resuspended in 60 μl of buffer B (10 mM HEPES, pH 7.9, 1.5 mM $MgCl_2$, 420 mM NaCl, 0.5 mM DTT, 0.2 mM EDTA, 25% glycerol, 0.5 mM PMSF). Samples were incubated for 20 min at 4°C and centrifuged at 10,000*g* for 15 min at 4°C. The supernate was transferred to a new tube, protein concentration was determined by the method of Bradford (31), and samples were stored at –80°C.

For the EMSA, the oligonucleotide containing the consensus sequence for NF-κB, OCT-1, or CREB was end labeled with [γ-^{32}P] ATP using T4 polynucleotide kinase and purified using Chroma Spin-10 columns. Samples were incubated with the labeled oligonucleotide (20,000–

30,000 cpm) for 20 min at room temperature in 50 mM Tris-HCl buffer, pH 7.5, containing 20% glycerol, 5 mM $MgCl_2$, 2.5 mM EDTA, 2.5 mM DTT, 250 mM NaCl, and 0.25 mg/ml poly(dI-dC). The possibility that the flavonoids EC, CT, and DP-B could act in part by inhibiting the binding of the active dimer to the NF-κB consensus sequence was tested. Before the addition of the labeled nucleotide, nuclear fractions from cells treated only with PMA were incubated in the presence of varying concentrations of EC, CT, or DP-B (0.1–200 nM) for 30 min. The labeled oligonucleotide was added, and the incubation was done as described above. The products were separated by electrophoresis in a 4% nondenaturing polyacrylamide gel using 0.5× TBE (Tris/borate 45 mM, EDTA 1 mM) as the running buffer. The gels were dried, and the radioactivity was quantitated in a Phosphoimager 640 (Amersham Pharmacia Biotechnology).

Determination of IL-2

Cells (1.5×10^6) were preincubated in 1.5 ml medium in the absence or presence of 8.6 μM EC, 17.2 μM CT, or 17.2 μM DP-B for 6 h, added with PMA (100 ng/ml) and further incubated for 18 h. IL-2 released to the media was measured after separating the cells by centrifugation at 800*g* for 10 min. IL-2 was measured using the human-IL-2 ELISA assay following the manufacturer's protocols.

Western blot analysis

For the determination of IκBα, p50, and RelA, cells (20×10^6 cells) were collected and centrifuged at 800*g* for 10 min. The pellet was rinsed with PBS and resuspended in 200 μl of 50 mM HEPES buffer, pH 7.4, containing 150 mM NaCl, protease inhibitors, and 2% Igepal. The final concentration of the inhibitors was 0.5 mmol/l PMSF, 1 mg/l leupeptin, 1 mg/l pepstatin, 1.5 mg/l aprotinin, 2 mg/l bestatin, and 0.4 mM sodium pervanadate. Samples were exposed to one cycle of freezing and thawing, incubated at 4°C for 30 min, and centrifuged at 15,000*g* for 30 min. The supernatant was decanted, and the protein concentration was measured. For p-IκBα and p-IKKβ determinations, total fractions were obtained by incubation with SDS sample buffer (62.5 mM Tris-HCl, pH 6.8, 2% w/v SDS, 10% glycerol, 50 mM DTT, 0.01% w/v bromophenol blue) following the antibody manufacturer's protocols.

Aliquots of total and nuclear fractions containing 25–50 μg protein were separated by reducing 10–12.5% PAGE and were electroblotted to PVDF membranes. Molecular weight standards (Santa Cruz Biotechnology) were run simultaneously. For IκBα, p50, and RelA, membranes were blocked overnight in 5% nonfat milk and subsequently incubated in the presence of the corresponding antibodies (1:1000 dilution) for 90 min at 37°C. For p-IκBα and p-IKKβ, membranes were blocked with 5% nonfat milk for 1 h and incubated in the presence of the corresponding antibody (1:1000 dilution) in 5% BSA overnight at 4°C. After incubation, for 90 min at room temperature, in the presence of the secondary antibody (horseradish peroxidase-conjugated) (1:10,000 dilution), the conjugates were visualized by chemiluminescence detection in a Phosphoimager 640 (Amersham Pharmacia Biotechnology).

Determination of cell oxidants

Cell oxidant levels were evaluated using the DCDCDHF probe, which can cross the membrane, and after oxidation, is converted into a fluorescent compound. Cells (1×10^5) were preincubated in the absence or presence of 8.6 μM EC, 17.2 μM CT, or 17.2 μM DP-B for 24 h. Subsequently, cells were incubated with 100 ng/ml PMA for 2.5–30 min, centrifuged at 800*g* for 10 min, rinsed with warm PBS, and suspended in 200 μl of RPMI 1640 medium containing 10 μM DCDCDHF. After 30 min of incubation at 37°C, the media was removed and cells were rinsed with PBS and then incubated in 200 μl of PBS containing 0.1% Igepal. After a brief sonication and 30 min incubation with regular shaking, the fluorescence at 525 nm (λ_{exc}: 475 nm) was measured. To evaluate DNA content, we added 50 μM propidium iodide to the samples. After incubating for 20 min at room temperature, the fluorescence (λ_{exc}: 538, λ_{em}: 590) was measured. Results are expressed as the ratio DCDCDHF/propidium iodide fluorescent.

Molecular modeling

Model building and energy calculations of DP-B were carried out with MacroModel 7.0 and BatchMin 7.0 (32) installed on a Silicon Graphics O2 workstation (R10000, 320 MB RAM, 54 GB hard disk) under the Irix 6.5 operating system. The MM2* force field (the version of Allinger's MM2 force field as implemented in MacroModel) was used. By default, atomic partial charges were calculated from data in the molecular mechanics force field, which also uses distance-dependent dielectric electrostatics instead of the standard dipole-dipole electrostatics. The conformational search of DP-B was carried out following an optimized Monte Carlo protocol (33), both in vacuo and in water, the latter according to the semianalytical solvation treatment GB/SA (34). The electrostatic cut-off was set to 50 Å. For energy minimization, the conjugate gradient method was used, with a final gradient value of 0.05 kJ $Å^{-1}$ mol^{-1} (0.01 kcal $Å^{-1}$ mol^{-1}) as the criterion for convergence. After 5000 Monte Carlo steps, the resulting set of conformers were fully minimized. Those non-enantiomeric structures lying within a 20 $kJ.mol^{-1}$ window above the global minimum were compared. Spatial coordinates of NF-κB in complex with IgκB DNA (35) were taken from the Research Collaboratory for Structural Bioinformatics Protein Data Bank (PDB file 1VKX).

Statistical analysis

One-way ANOVA with subsequent post hoc comparisons by Scheffe were performed using Statview 512+ (Brainpower, Inc., Calabazas, CA). $P < 0.05$ was considered statistically significant. Values are given as means ± SE.

RESULTS

Variations in extracellular EC, CT, or DP-B concentrations affect their cellular content

To assess whether EC, CT, and DP-B accumulated in the cells and whether the DP-B was cleaved to monomers, we measured the cellular concentration of these flavonoids. After 24 h incubation with varying concentrations of EC, CT, or DP-B, the concentrations of EC, CT, and DP-B were measured in total cell fractions and in nuclear fractions. EC, CT, and DP-B accumulated in the cells in a dose-dependent manner (Fig. 1). At the same extracellular

concentrations, significantly higher amounts ($P<0.05$) of cellular EC and CT were observed compared with DP-B. In the cells pretreated with DP-B, while the compound was transported inside the cell, negligible amounts of monomers were detected, suggesting that only minimal amounts of the DP-B were cleaved under the conditions used. A dose-dependent accumulation of EC and DP-B in the nuclear fraction was observed, whereas CT was undetectable under the present experimental conditions (Fig. 1).

EC, CT, and DP-B inhibit NF-κB nuclear binding activity and IL-2 production

The DNA binding activity of NF-κB was measured by EMSA in nuclear extracts isolated from Jurkat cells pretreated without or with EC, CT, or DP-B for 24 h, and subsequently treated with 100 ng/ml PMA. The specificity of the NF-κB-DNA binding was assessed by competition with a 100-fold molar excess of unlabeled oligonucleotide containing the consensus sequence for either NF-κB or OCT-1 (Fig. 2*A*). The members of the Rel/NF-κB proteins present in the active NF-κB in Jurkat cells were characterized by an EMSA supershift assay (Fig. 2*A*). EC, CT, and DP-B inhibited, between 30 min and 4 h, PMA-induced NF-κB binding activity (data not shown). After 4 h exposure to PMA, a dose-response inhibition was observed for EC, CT, and DP-B. Figure 2*B* depicts the dose (1.7–17.2 μM)-dependent inhibition of NF-κB binding activity for the dimeric fraction. The lowest DNA binding activity was observed at concentrations of 8.6 μM EC, 17.2 μM CT, and 17.2 μM DP-B (65, 64, and 75% reduction, respectively), compared with that observed in control cells treated with PMA only (Fig. 2*C*).

The inhibition of a PMA-induced increase in NF-κB DNA binding activity could result in a reduced transactivation of NF-κB-driven genes. The expression of IL-2 was evaluated by measuring the release of IL-2 to the media using an ELISA assay. IL-2 production by nonstimulated cells was below the level of detection; PMA stimulation resulted in a robust stimulation of IL-2 production. PMA-induced production of IL-2 protein levels was decreased by 53, 48, and 59% in the cells pretreated with 8.6 μM EC, 17.2 μM CT, and 17.2 μM DP-B, respectively, compared with IL-2 production in cells treated with PMA only (Fig. 3).

EC, CT, and DP-B inhibit PMA-induced IκBα and IKKβ phosphorylation

To investigate at which steps EC, CT, and DP-B inhibit the NF-κB activation cascade, we measured the phosphorylation and concentration of the inhibitory peptide IκBα. One of the required steps in the activation of NF-κB is the phosphorylation and further degradation of the IκB peptides that prevent the translocation of the active NF-κB into the nucleus. IκBα concentration and phosphorylation were determined by Western blot in total cell fractions (Fig. 4*A*). After addition of PMA, the phosphorylation of IκBα (measured as the ratio p-IκBα/IκBα) revealed a maximum value after 10 min of incubation, followed by a steady decrease for the following 230 min (Fig. 4*B*). After 10 min incubation with PMA, the ratio p-IκBα/IκBα was 32, 28, and 31% lower in the cells preincubated with 8.6 μM EC, 17.2 μM CT, and 17.2 μM DP-B, respectively, compared with the cells incubated with PMA alone (Fig. 4*C*).

Because the phosphorylation of IκBα was found to be inhibited with the flavonoids tested, we characterized an upstream event in the NF-κB activation cascade by measuring IKKβ phosphorylation. The kinetics of IKKβ phosphorylation showed a maximum value after 2.5 min

of PMA addition (data not shown). In the cells pretreated with 17.2 μM DP-B, a 47% inhibition in IKKβ phosphorylation was observed after 2.5 min incubation with PMA, compared with the control group (Fig. 4*A*, 4*C*). After 2.5 min incubation with PMA, IKKβ phosphorylation was inhibited by 8.6 μM EC and 17.2 μM CT (51 and 42%, respectively) (Fig. 4*C*).

EC, CT, and DP-B prevents a PMA-induced increase in cell oxidants

One of the signals that leads to the activation of the NF-κB pathway is an increase in intracellular oxidants. To assess whether EC, CT, or DP-B could blunt PMA-induced NF-κB activation by acting as antioxidants, we tested the capacity of these compounds to prevent oxidative stress. After 2.5 min of incubating cells in the presence of PMA, an increase in cell oxidant levels, measured with the probe DCDCDHF, was observed. This increase was markedly inhibited in cells previously treated with 8.6 μM EC, 17.2 μM CT, and 17.2 μM DP-B for 24 h (Fig. 5) at all the times measured (2.5–30 min).

EC, CT, and DP-B partially act by blocking NF-κB binding to DNA

The concentrations of p50 and RelA (components of the active dimer) were measured by Western blot in the nuclear fractions after incubation with PMA. PMA induced a significant increase in RelA and p50 nuclear content. Figure 6*A* depicts the kinetics of p50 and RelA nuclear levels (0–4 h after PMA addition) in cells pretreated with DP-B. The concentration of p50 and RelA was higher (30 min to 4 h) in the cells treated with PMA compared with nonstimulated cells. Cells preincubated with DP-B for 24 h and treated with PMA had lower levels of p50 and Rel A after 30 min of PMA addition, reaching values similar to those observed for PMA after 4 h of incubation. Similar results were obtained for EC and CT (data not shown). After 4 h of PMA stimulation, no significant differences were observed in the nuclear concentrations of p50 or RelA in cells preincubated with EC, CT, or DP-B compared with the PMA group (Fig. 6*B*).

Based on these results, we investigated whether the low nuclear binding of NF-κB to DNA found in the cells treated with EC, CT, or DP-B could be due to a direct inhibition of the binding of the active NF-κB to the κB sites. Nuclear fractions isolated from cells incubated in the absence of flavonoids and treated with PMA for 4 h were added during the binding reaction with variable concentrations of DP-B (0.1–100 nM) (Fig. 7*A*), EC (0.2–200 nM), or CT (0.2–200 nM) for 30 min. The addition of 20 nM EC, 20 nM CT, or 10 nM DP-B reduced (78, 81, and 78%, respectively) the binding of the active NF-κB to DNA (Fig. 7*B*). DP-B did not affect the DNA binding of the transcription factors OCT-1 and CREB (Fig. 7*C*).

DISCUSSION

In the present study, we investigated possible mechanisms involved in the inhibition of NF-κB by the monomeric flavan-3-ols, EC and CT, and a dimeric fraction DP-B isolated from cocoa. A first step was to investigate whether EC, CT, and DP-B were incorporated in Jurkat T cells and to characterize their distribution in cytosolic and nuclear fractions. We observed that the three compounds accumulate in the cells to a different extent: EC > CT > DP-B. Although there was a lower uptake of DP-B compared with EC and CT, the ratio for nuclear content/total cell content was 10 times higher in the cells treated for 24 h in the presence of DP-B compared with EC

(0.355 and 0.036, respectively, at 17.2 μM added flavonoid). This indicates a selective accumulation of DP-B in the nuclei compared with the monomers.

Flavonoids have previously been shown to inhibit transcription factor NF-κB and the expression of NF-κB-regulated genes (36). (–)-Epigallocatechin gallate, the major polyphenol in tea, inhibited in vitro and in vivo lipopolysaccharide-induced tumor necrosis factor α (TNF-α) secretion (37). Pretreatment of RAW 264.7 cells for 2 h in the presence of 100 mM epigallocatechin gallate prevented lipopolysaccharide-induced increases in NF-κB nuclear binding activity (37). Oroxylin A, a flavonoid isolated from Chinese herbs, inhibited NF-κB and the expression of two NF-κB-regulated genes, cyclooxygenase-2 and inducible nitric oxide synthase (38). EC, CT, and dimers B1 and B2 (at 344 and 173 μM concentrations, for monomers and dimers, respectively) inhibited the interferon γ-induced expression of NF-κB-dependent genes in RAW 264.7 macrophages (23). All of these compounds markedly inhibited the secretion of TNF-α, whereas the monomers, and to a lesser extent the dimers, inhibited the expression of an NF-κB-driven luciferase reporter gene (23). In line with these results, we observed a significant inhibition (48–59%) of PMA-induced IL-2 secretion at concentrations as low as 8.6 and 17.2 μM monomer and dimer, respectively. Treatment with EC, CT, and DP-B also resulted in the inhibition of the constitutive NF-κB binding activity (data not shown).

The inhibitory peptide IκBα (one member of the inhibitory IκB proteins) binds to NF-κB and prevents the translocation of the active NF-κB to the nuclei and its binding to DNA. During NF-κB activation, IκBα is phosphorylated by the serine-specific IKK, with posterior ubiquitinization and degradation of IκBα by the proteasome (20). We observed a lower ratio of p-IκBα/IκBα after 10 min incubation with PMA in cells preincubated with EC, CT, and DP-B compared with control cells. The upstream step, the phosphorylation of IKK, is activated by PMA via IKKβ (39, 40). The concentration of p-IKKβ after 2.5 min incubation with PMA was lower in the cells pretreated with EC, CT, or DP-B than in controls. These observations indicate that these flavonoids partially inhibit PMA-induced NF-κB activation by preventing IKKβ phosphorylation. In agreement with our results, the flavonoid silibinin has been shown to inhibit constitutive IKKα in intact DU145 prostate carcinoma cells, as well as through a direct inhibition of immunoprecipitated IKKα (41). Furthermore, it has been reported that some tea polyphenols can inhibit the proteasome activity with consequent accumulation of IκBα protein (42). Inhibition of the early steps in the NF-κB activation cascade could be partially mediated by the well-described antioxidant action of EC, CT, and DP-B (13), because we observed that these flavonoids inhibited PMA-induced increase in the steady-state level of cell oxidants. Oxygen and nitrogen active species and changes in cell thiol redox state have been shown to activate NF-κB in different primary cell cultures and cell lines (See refs 16 and 43–47 for reviews). For example, in primary human chondrocytes, IL-1β induced NO production and activated NF-κB (48). Epigallocatechin-3-gallate diminished NO cellular concentrations and the expression of NF-κB-target genes (48). Similarly, in RAW 264.7 macrophages stimulated with interferon-γ, different flavonoids inhibited NO production and NF-κB-dependent transcriptional activity (23). However, other mechanisms of action, such as a direct effect of EC, CT, and DP-B on IKK, could also be operating.

After 4 h incubation with PMA, the ratio p-IkBα/IkBα was similar in cells pretreated or not with EC, CT, or DP-B, and similar p50 and RelA nuclear concentrations were observed. However, a lower NF-κB nuclear binding activity was found in the cells pretreated with EC, CT, and DP-B. This finding, and the observed accumulation of EC and DP-B in the nuclei, led us to propose that these flavonoids have the capacity to interact with the active NF-κB, preventing its binding to the κB site. Supporting this hypothesis we observed that the addition of EC, CT, and DP-B, in nanomolar concentrations, to nuclear fractions isolated from PMA-stimulated cells resulted in a dose-dependent inhibition of NF-κB binding to its consensus sequence. DP-B, at 0.1 nM, resulted in a 51% inhibition in NF-κB binding. Under similar experimental conditions, DP-B did not affect the DNA binding of transcription factors OCT-1 and CREB, indicating a selective effect of DP-B on the binding of NF-κB to its DNA consensus sequence.

Based on the above findings, a molecular model of how DP-B might interact with NF-κB proteins was constructed using MacroModel 7.0 (32). The procedures used were the following: (i) Conformational searches in vacuo and in water carried out with an optimized Monte Carlo procedure (33) produced a very similar ensemble of conformers where a common structure predominates (see below); (ii) fitting of the minimum energy conformer found at the previous step onto the base-specific binding residues (Arg 54 and Arg 56 of p50, and Arg 33 and Arg 35 of RelA) of NF-κB (PDB entry 1VKX) was achieved by manual docking.

A molecular model of DP-B was initially constructed using the model-building facility implemented in MacroModel. Coordinates of this structure were later used as input for BatchMin, the calculation module of this program. To search the conformational space available to this compound, an optimized Monte Carlo procedure was run, which allows free rotation around dihedral angles that constitute the major determinants of the structure, that is, ϕ1, ϕ2, and ϕ3 for DP-B (Fig. 8*A*). Values for these angles in the conformer corresponding to the global minimum are listed in the legend to Figure 8, and a graphical rendering is shown in Figure 8*B*. This represents a folded structure where ring B' stacks onto ring A, orienting the hydroxyl groups toward the same edge of the molecule.

Figure 9 depicts the superimposition of the base-specific guanines of the κB-DNA consensus sequence and DP-B, and their interaction through hydrogen bonds with the pairs of Arg residues present in the DNA binding region of both p50 (Arg 54 and Arg 56) and RelA (Arg 33 and Arg 35). Stacked rings B' and A of DP-B lie very close to the positions occupied by the two guanines rings (0.41 and 0.47 Å RMS deviation for the guanine pairs binding p50 and RelA, respectively). Moreover, the polar atoms of DP-B are favorably placed for giving rise to a similar hydrogen bonding pattern to that observed in the complex (Fig. 9). Overall, in both cases, DP-B seems to behave as a very reasonable mimic of the guanine pairs. To a lesser extent, this situation could be extended to EC and CT, both compounds sharing the same hydrogen bonding group distribution critical for binding but lacking the covalent bridge present in DP-B.

A molecular surface representation of NF-κB colored by the electrostatic potential is depicted in Figure 10. Onto this surface the putative binding sites for DP-B are shown. Two molecules of DP-B were docked in place of the two pairs of consecutive guanines present in the κB-DNA recognition sequence. The following consistency tests were adopted to validate the model (49): (i) Translation of the ligand to a large distance (100 Å) away from the binding site produces an

increase in excess of 120 kJ.mol^{-1} in the calculated energy of the ligand-protein pair; (ii) there is hardly any spatial overlap between DP-B and the amino acid residues involved in the interaction, as evaluated by measuring the volume common to both (~1%). Furthermore, this model shows that the interaction between DP-B and NF-κB is possible simultaneously at the two sites where the two Arg pairs occur, that is, no steric hindrance between the ligands takes place.

The crystal structure of NF-κB bound to DNA (35) shows the presence of two consecutive guanines in the κB site that are essential for the base-specific binding in both p50 and RelA of the active NF-κB to its cognate sequence. Arg 54 and Arg 56 of p50 as well as Arg 33 and Arg 35 of RelA are the residues interacting with the guanines –4 and –3 as well as +3 and +4, respectively (35). The global minimum energy conformer of DP-B is proposed here as a mimic for the guanine-guanine pair. Consistently, none of the two other transcription factors tested (OCT-1 and CREB) presents two consecutive guanines in their DNA consensus motifs. Because both pairs of Arg present in p50 and RelA are essential for the base-specific contact, binding of DP-B to these residues would prevent its interaction with DNA. To further characterize the binding mechanisms, molecular dynamics of DP-B bound to NF-κB and in vitro competition experiments are needed to further confirm this hypothesis.

The present work demonstrates that the previously observed inhibition of IL-2 and IL-1β production by cocoa procyanidins can be attributed in part to inhibition of the NF-κB activation cascade (24, 25). T-cell activation is an important step in the initiation of the immunological response. Normally, T cells do not contain constitutive levels of IL-2 (50). However, stimulation of T cells by PMA activates a cascade of signaling events, including the up-regulation of transcription factors, such as NF-κB and NF-AT, all leading to the transcription and secretion of IL-2 (51, 52). Thus, regulation of IL-2 at the level of transcription is critically involved in the control of T-cell expansion and in the normal immune response (50, 53). In this context, the regulation of NF-κB by the flavan-3-ols, EC and CT, and DP-B may contribute to the reported anti-inflammatory and immunomodulatory actions proposed for these compounds.

Note that the flavonol and dimer concentrations used in this study represent physiological concentration for the oral cavity and gut (53). Similarily, the monomer concentrations used are reflective of concentrations reported for blood. Although the dimer concentrations used are higher than those typically found in blood after the consumption of flavonoid-rich foods, these concentrations could theorically be approached if the dimer were given as a pharmaceutical.

In summary, the flavanols, EC and CT, and the B-type dimeric oligomers can regulate the immune response in part by modulating the oxidant-responsive transcription factor NF-κB. This modulation can occur at the early steps of the NF-κB activation cascade, that is, regulation of oxidant levels, IKK activation, and subsequent IκBα phosphorylation, and at later stages, through a direct interaction of EC, CT, and DP-B with NF-κB proteins inhibiting the binding of active NF-κB to κB sites.

ACKNOWLEDGMENTS

This work was supported by grants (B054 and BO42) from the University of Buenos Aires, Argentina; Mars, Inc., Hackettstown, NJ; the National Institutes of Health (DK35747), Bethesda, MD. G. G. Mackenzie is a fellow from the University of Buenos Aires, Argentina.

REFERENCES

1. Santos-Buelga, C., and Scalbert, A. (2000) Proanthocyanidins and tannin-like compounds: nature, occurance, dietary intake and effects in nutrition and health. *J. Food Sci. Agric.* **80,** 1094–1117

2. Weisburger, J. H. (2001) Chemopreventive effects of cocoa polyphenols on chronic diseases. *Exp. Biol. Med. (Maywood)* **226,** 891–897

3. Kris-Etherton, P. M., and Keen, C. L. (2002) Evidence that the antioxidant flavonoids in tea and cocoa are beneficial for cardiovascular health. *Curr. Opin. Lipidol.* **13,** 41–49

4. Taubert, D., Berkels, R., Roesen, R., and Klaus, W. (2003) Chocolate and blood pressure in elderly individuals with isolated systolic hypertension. *JAMA* **290,** 1029–1030

5. Heiss, C., Dejam, A., Kleinbongard, P., Schewe, T., Sies, H., and Kelm, M. (2003) Vascular effects of cocoa rich in flavan-3-ols. *JAMA* **290,** 1030–1031

6. Holt, R. R., Schramm, D. D., Keen, C. L., Lazarus, S. A., and Schmitz, H. H. (2002) Chocolate consumption and platelet function. *JAMA* **287,** 2212–2213

7. Rice-Evans, C. (2001) Flavonoid antioxidants. *Curr. Med. Chem.* **8,** 797–807

8. Adamson, G. E., Lazarus, S. A., Mitchell, A. E., Prior, R. L., Cao, G., Jacobs, P. H., Kremers, B. G., Hammerstone, J. F., Rucker, R. B., Ritter, K. A., et al. (1999) HPLC method for the quantification of procyanidins in cocoa and chocolate samples and correlation to total antioxidant capacity. *J. Agric. Food Chem.* **47,** 4184–4188

9. Hammerstone, J. F., Lazarus, S. A., and Schmitz, H. H. (2000) Procyanidin content and variation in some commonly consumed foods. *J. Nutr.* **130,** 2086S–2092S

10. Waterhouse, A. L., Shirley, J. R., and Donovan, J. L. (1996) Antioxidants in chocolate. *Lancet* **348,** 834

11. Kondo, K., Hirano, R., Matsumoto, A., Igarashi, O., and Itakura, H. (1996) Inhibition of LDL oxidation by cocoa. *Lancet* **348,** 1514

12. Lotito, S. B., and Fraga, C. G. (1998) (+)-Catechin prevents human plasma oxidation. *Free Radic. Biol. Med.* **24,** 435–441

13. Lotito, S. B., Actis-Goretta, L., Renart, M. L., Caligiuri, M., Rein, D., Schmitz, H. H., Steinberg, F. M., Keen, C. L., and Fraga, C. G. (2000) Influence of oligomer chain length on the antioxidant activity of procyanidins. *Biochem. Biophys. Res. Commun.* **276,** 945–951

14. Sanbongi, C., Susuki, N., and Sakane, T. (1997) Polyphenols in chocolate, which have antioxidant activity, modulate immune functions in humans in vitro. *Cell. Immunol.* **177,** 129–136

15. Pahl, H. L. (1999) Activators and target genes of Rel/NF-κB transcription factors. *Oncogene* **18,** 6853–6866

16. Ginn-Pease, M. E., and Whisler, R. L. (1998) Redox signals and NF-kappaB activation in T cells. *Free Radic. Biol. Med.* **25,** 346–361

17. Baeuerle, P. A., and Baltimore, D. (1988) I kappa B: a specific inhibitor of the NF-kappa B transcription factor. *Science* **242,** 540–546

18. Delhase, M., Hayakawa, M., Chen, Y., and Karin, M. (1999) Positive and negative regulation of I kappa B kinase activity through IKK beta subunit phosphorylaation. *Science* **284,** 309–313

19. Senftleben, U., and Karin, M. (2002) The IKK/NF-κB pathway. *Crit. Care Med.* **30,** S18–S26

20. Karin, M. (1999) How NF-κB is activated: the role of the IκB kinase (IKK) complex. *Oncogene* **18,** 6867–6874

21. Mackenzie, G. G., Zago, M. P., Keen, C. L., and Oteiza, P. I. (2002) Low intracellular zinc impairs the translocation of activated NF-kappa B to the nuclei in human neuroblastoma IMR-32 cells. *J. Biol. Chem.* **277,** 34610–34617

22. Rosette, C., and Karin, M. (1995) Cytoskeletal control of gene expression: depolymerization of microtubules activates NF-kappa B. *J. Cell Biol.* **128,** 1111–1119

23. Park, Y. C., Rimbach, G., Saliou, G., Valacchi, G., and Packer, L. (2000) Activity of monomeric, dimeric, and trimeric flavonoids on NO production, TNF-alpha secretion, and NF-kappaB-dependent gene expression in RAW 264.7 macrophages. *FEBS Lett.* **465,** 93–97

24. Mao, T. K., Powell, J. J., Van de Water, J., Keen, C. L., Schmitz, H. H., and Gershwin, M. E. (1999) The influence of cocoa procyanidins on the transcription of interleukin-2 in peripheral blood mononuclear cells. *Int. J. Immunotheraphy* **XV,** 23–29

25. Mao, T. K., Powell, J. J., Van de Water, J., Keen, C. L., Schmitz, H. H., Hammerstone, M., and Gershwin, M. E. (2000) The effect of cocoa procyanidins on the transcription and secretion of interleukin 1 beta in peripheral blood mononuclear cells. *Life Sci.* **66,** 1377–1386

26. Mao, T. K., Powell, J. J., Van de Water, J., Keen, C. L., Schmitz, H. H., and Gershwin, M. E. (2000) Effect of cocoa procyanidins on the secretion of Interleukin-4 in peripheral blood mononuclear cells. *J. Med. Food* **3,** 107–114

27. Holt, R. R., Lazarus, S. A., Sullards, M. C., Zhu, Q. Y., Schramm, D. D., Hammerstone, J. F., Fraga, C. G., Schmitz, H. H., and Keen, C. L. (2002) Procyanidin dimer B2 [epicatechin-(4beta-8)-epicatechin] in human plasma after the consumption of a flavanol-rich cocoa. *Am. J. Clin. Nutr.* **76,** 798–804

28. Rein, D., Lotito, S., Holt, R. R., Keen, C. L., Schmitz, H. H., and Fraga, C. G. (2000) Epicatechin in human plasma: in vivo determination and effect of chocolate consumption on plasma oxidation status. *J. Nutr.* **130,** 2109S–2114S

29. Osborn, L., Kunkel, S., and Nabel, G. J. (1989) Tumor necrosis factor alpha and interleukin 1 stimulate the human immunodeficiency virus enhancer by activation of the nuclear factor kappa B. *Proc. Natl. Acad. Sci. USA* **86,** 2336–2340

30. Dignam, J. D., Lebovitz, R. M., and Roeder, R. G. (1983) Accurate transcription initiation by RNA polymerase II in a soluble extract from isolated mammalian nuclei. *Nucleic Acids Res.* **11,** 1475–1489

31. Bradford, M. M. (1976) A rapid and sensitive method for the quantitation of microgram quantities of protein utilizing the principle of protein-dye binding. *Anal. Biochem.* **72,** 248–254

32. Mohamadi, F., Richards, N. G., Guida, W. C., Liskamp, M., Lipton, M., Caufield, C., Chang, G., Hendrickson, T., and Still, W. C. (1990) Macro-Model-an integrated software system for modeling organic and bioorganic molecules using molecular mechanisms. *J. Comput. Chem.* **11,** 440–467

33. Chang, G., Guida, W. C., and Still, W. C. (1989) An internal coordinate Monte Carlo Method for searching conformational space. *J. Am. Chem. Soc.* **111,** 4379–4386

34. Still, W. C., Temoczyk, A., Hawley, R. C., and Hendrickson, T. (1990) Semi analytical treatment of solvation for molecular mechanics and dynamics. *J. Am. Chem. Soc.* **112,** 6627

35. Chen, F. E., Huang, D. B., Chen, Y. Q., and Ghosh, G. (1998) Crystal structure of p50/p65 heterodimer of transcription factor NF-kappaB bound to DNA. *Nature* **391,** 410–413

36. Saliou, C., Valacchi, G., and Rimbach, G. (2001) Assessing bioflavonoids as regulators of NF-kappa B activity and inflammatory gene expression in mammalian cells. *Methods Enzymol.* **335,** 380–387

37. Yang, F., de Villiers, W. J., McClain, C. J., and Varilek, G. W. (1998) Green tea polyphenols block endotoxin-induced tumor necrosis factor-production and lethality in a murine model. *J. Nutr.* **128,** 2334–2340

38. Chen, Y., Yang, L., and Lee, T. J. (2000) Oroxylin A inhibition of lipopolysaccharide-induced iNOS and COX-2 gene expression via suppression of nuclear factor-kappaB activation. *Biochem. Pharmacol.* **59,** 1445–1457

39. Ren, H., Schmalstieg, A., van Oers, N. S., and Gaynor, R. B. (2002) I-kappa B kinases alpha and beta have distinct roles in regulating murine T cell function. *J. Immunol.* **168,** 3721–3731

40. Lallena, M. J., Diaz-Meco, M. T., Bren, G., Paya, C. V., and Moscat, J. (1999) Activation of IkappaB kinase beta by protein kinase C isoforms. *Mol. Cell. Biol.* **19,** 2180–2188

41. Dhanalakshmi, S., Singh, R. P., Agarwal, C., and Agarwal, R. (2002) Silibinin inhibits constitutive and TNFalpha-induced activation of NF-kappaB and sensitizes human prostate carcinoma DU145 cells to TNFalpha-induced apoptosis. *Oncogene* **21,** 1759–1767

42. Nam, S., Smith, D. M., and Ping Dou, Q. (2001) Ester Bond-containing Tea Polyphenols Potently Inhibit Proteasome Activity in Vitro and in Vivo. *J. Biol. Chem.* **276,** 13322–13330

43. Bowie, A., and O'Neill, L. A. (2000) Oxidative stress and nuclear factor-kappaB activation: a reassessment of the evidence in the light of recent discoveries. *Biochem. Pharmacol.* **59,** 13–23

44. Li, N., and Karin, M. (1999) Is NF-κB the sensor of oxidative stress? *FASEB J.* **13,** 1137–1143

45. Sen, C. K., and Packer, L. (1996) Antioxidant and redox regulation of gene transcription. *FASEB J.* **10,** 709–720

46. Moran, L. K., Gutteridge, J. M., and Quinlan, G. J. (2001) Thiols in cellular redox signalling and control. *Curr. Med. Chem.* **8,** 763–772

47. Arrigo, A. P. (1999) Gene expression and the thiol redox state. *Free Radic. Biol. Med.* **27,** 936–944

48. Singh, R., Ahmed, S., Islam, N., Goldberg, V. M., and Haqqi, T. M. (2002) Epigallocatechin-3-gallate inhibits interleukin-1beta-induced expression of nitric oxide synthase and production of nitric oxide in human chondrocytes: suppression of nuclear factor kappaB activation by degradation of the inhibitor of nuclear factor kappaB. *Arthritis Rheum.* **46,** 2079–2086

49. Arighi, C. N., Rossi, J. P., and Delfino, J. M. (1998) Temperature-induced conformational transition of intestinal fatty acid binding protein enhancing ligand binding: a functional, spectroscopic, and molecular modeling study. *Biochemistry* **37,** 16802–16814

50. Smith, K. A. (1988) Interleukin-2: inception, impact, and implications. *Science* **240,** 1169–1176

51. Han, S. H., Yea, S. S., Jeon, Y. J., Yang, K. H., and Kaminski, N. E. (1998) Transforming growth factor-beta 1 (TGF-beta1) promotes IL-2 mRNA expression through the up-regulation of NF-kappaB, AP-1 and NF-AT in EL4 cells. *J. Pharmacol. Exp. Ther.* **287,** 1105–1112

52. Zhao, W., Schafer, R., and Barnett, J. B. (1999) Propanil affects transcriptional and posttranscriptional regulation of IL-2 expression in activated EL-4 cells. *Toxicol. Appl. Pharmacol.* **154,** 153–159

53. Leonard, W. J., Kronke, M., Peffer, N. J., Depper, J. M., and Greene, W. C. (1985) Interleukin 2 receptor gene expression in normal human T lymphocytes. *Proc. Natl. Acad. Sci. USA* **82,** 6281–6285

54. Nicholls, A., Sharp, K. A., and Honig, B. (1991) Protein folding and association: insights from the interfacial and thermodynamic properties of hydrocarbons. *Proteins* **11,** 281–296

Received May 29, 2003; accepted October 1, 2003.

Fig. 1

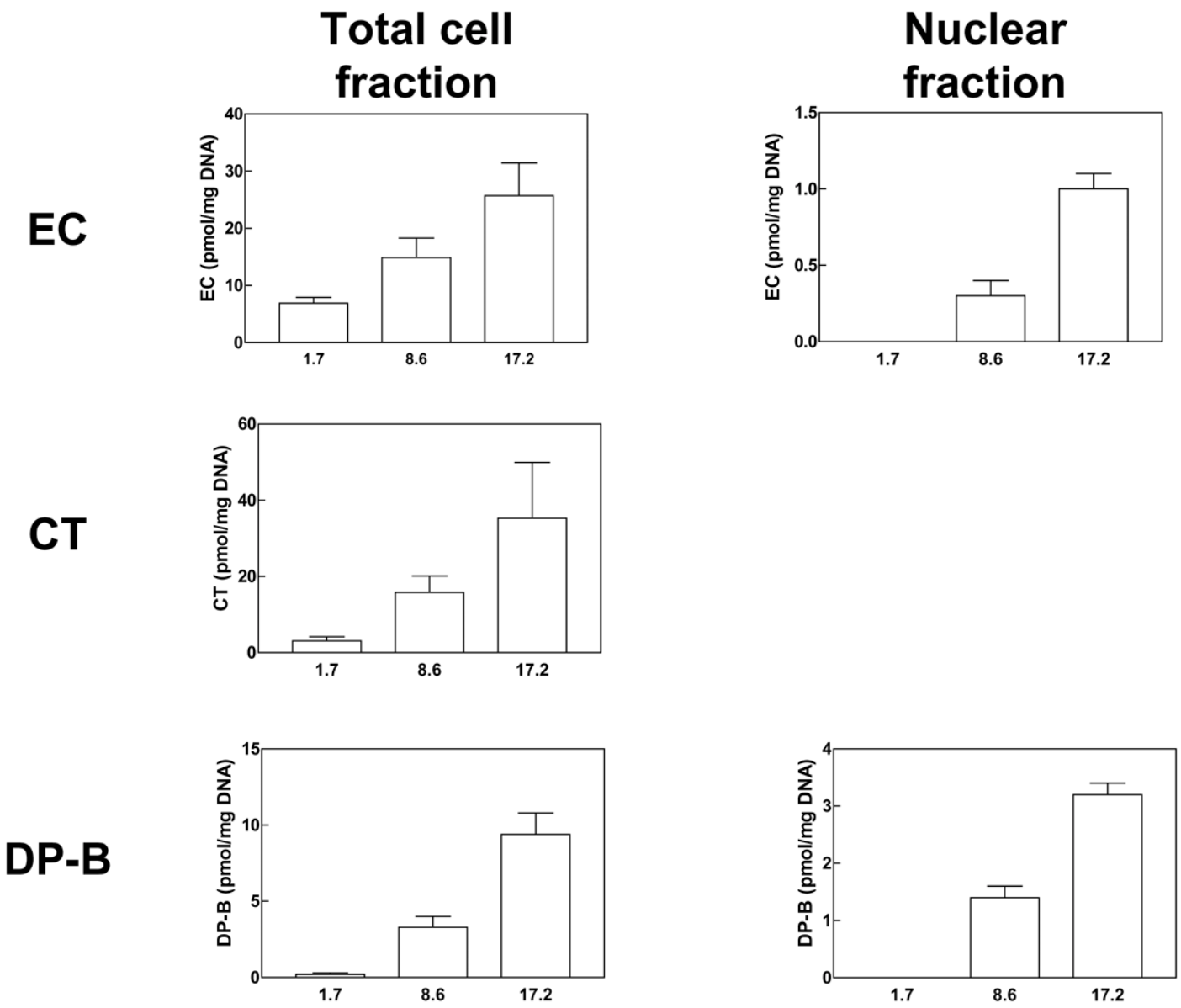

Figure 1. Cellular concentrations of EC, CT, and DP-B. Cells were incubated in the presence of EC, CT, or DP-B (1.7–17.2 μM) for 24 h. After isolation of total and nuclear fractions as described in Materials and Methods, concentrations of EC, CT, and DP-B in total cell fractions and in nuclear fractions were measured. Results are shown as means ± SE of four independent experiments.

Fig. 2

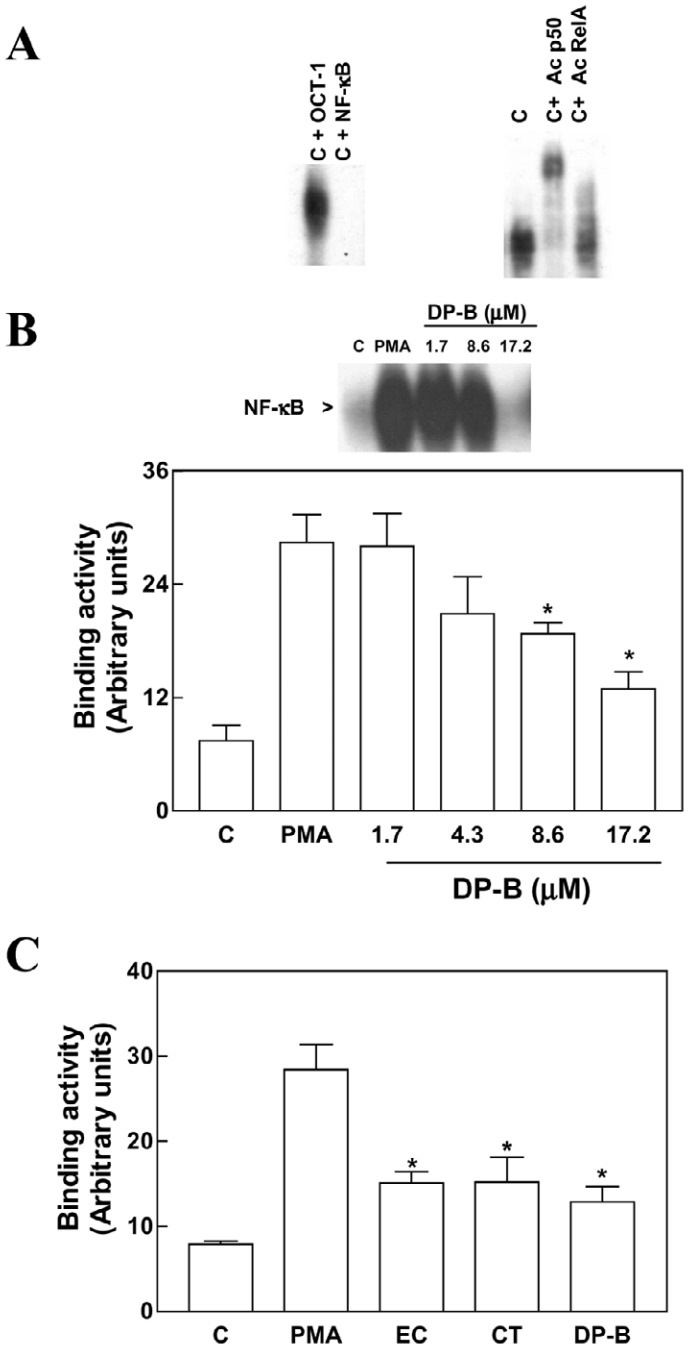

Figure 2. NF-κB-DNA binding activity in nuclear fractions from Jurkat cells. Fractions were isolated after 24 h of preincubation in the absence (control, C) or in the presence of 1.7–17.2 μM EC, CT, or DP-B and a further 4 h incubation without (C) or with (PMA [control cells incubated with PMA], EC, CT, DP-B) 100 ng/ml PMA. ***A)*** To determine the specificity of the NF-κB-DNA complex, a control (C) sample was incubated in the presence of a 100-fold molar excess of unlabeled oligonucleotide containing the consensus sequence for either NF-κB or OCT-1 before the binding assay (left panel). To determine the protein components of the active NF-κB, we incubated control samples in the presence of antibodies for p50 or RelA before the binding assay (right panel). ***B)*** EMSA of nuclear fractions incubated with different concentrations of DP-B. Bands were quantitated as described in Materials and Methods; results are shown as means ± SE of six independent experiments. *Significantly different compared with the PMA group (P<0.001, one way ANOVA test). ***C)*** Effect of 8.6 μM EC, 17.2 μM CT, and 17.2 μM DP-B on NF-κB-DNA binding activity. Results are shown as means ± SE of four independent experiments. *Significantly different compared with the PMA group (P<0.01, one-way ANOVA).

Fig. 3

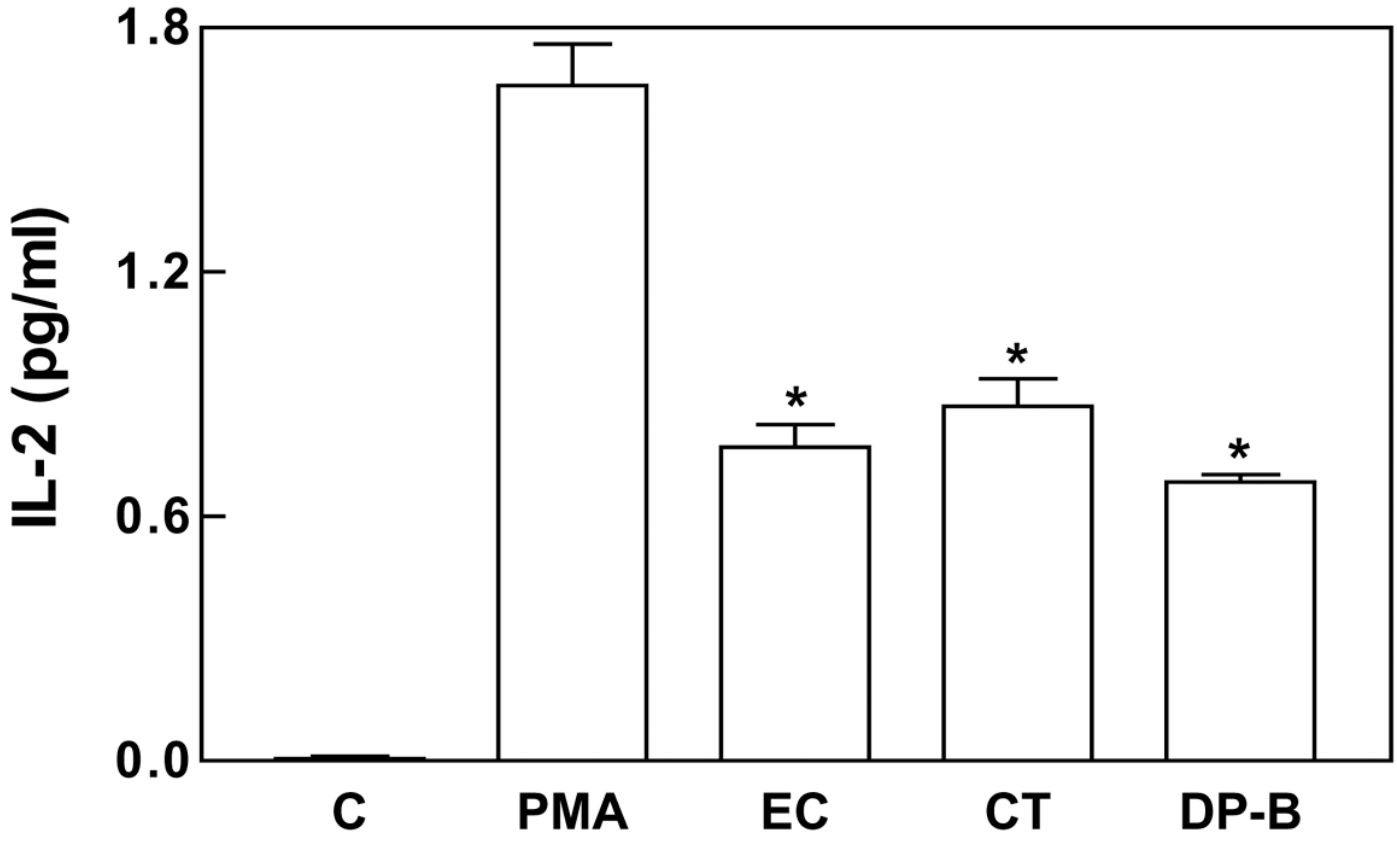

Figure 3. EC, CT, and DP-B inhibit IL-2 release in Jurkat cells. Cells were preincubated in the absence or presence of 8.6 μM EC, 17.2 μM CT, or 17.2 μM DP-B for 24 h followed by 18 h incubation without (control, C) or with (PMA [control cells incubated with PMA], EC, CT, DP-B) 100 ng/ml PMA. Results are shown as means ± SE of four independent experiments. *Significantly different compared with the PMA control group (P<0.001, one way ANOVA).

Fig. 4

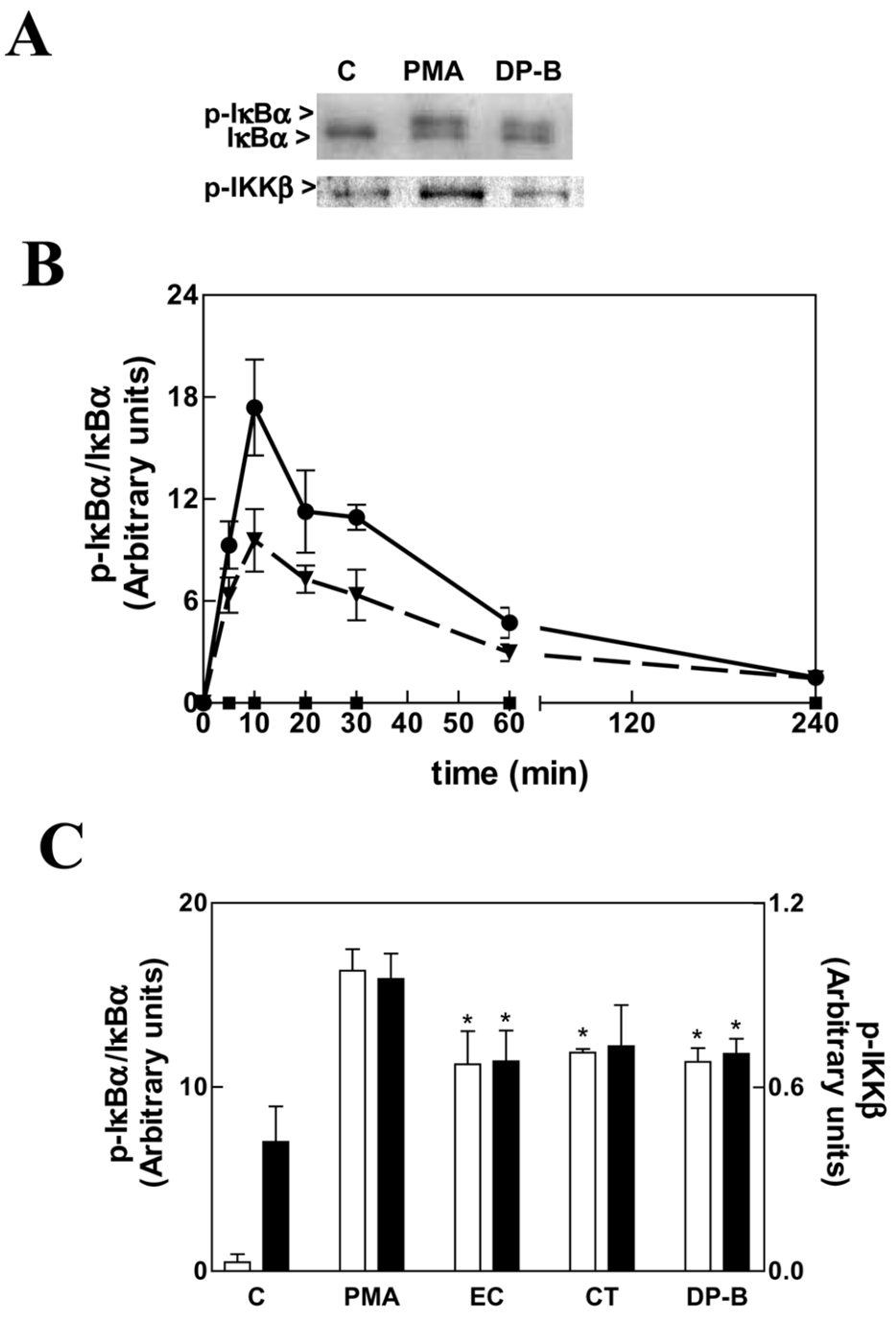

Figure 4. p-IκBα, IκBα, and p-IKKβ levels in total fractions isolated from Jurkat cells. Fractions were isolated after 24 h of preincubation in the absence (control, C) or presence of 8.6 μM EC, 17.2 μM CT, or 17.2 μM DP-B and a further incubation without (C) or with (PMA [control cells incubated with PMA], EC, CT, DP-B) 100 ng/ml PMA for 2.5–240 min. ***A)*** Western blots for p-IκB and IκBα after 10 min, and p-IKKβ after 2.5 min incubation with PMA. ***B)*** Kinetics of the changes in the ratio p-IκBα/IκBα for C (■), PMA (●), and DP-B (▼) cells. Results are shown as means ± SE of four independent experiments. ***C)*** Ratio p-IκBα/IκBα (empty bars) after 10 min, and p-IKKβ (full bars) after 2.5 min of incubation with PMA in cells previously treated for 24 h with 8.6 μM EC, 17.2 μM CT, or 17.2 μM DP-B. Results are shown as means ± SE of four independent experiments. *Significantly different compared with the PMA control group (P<0.05, one-way ANOVA).

Fig. 5

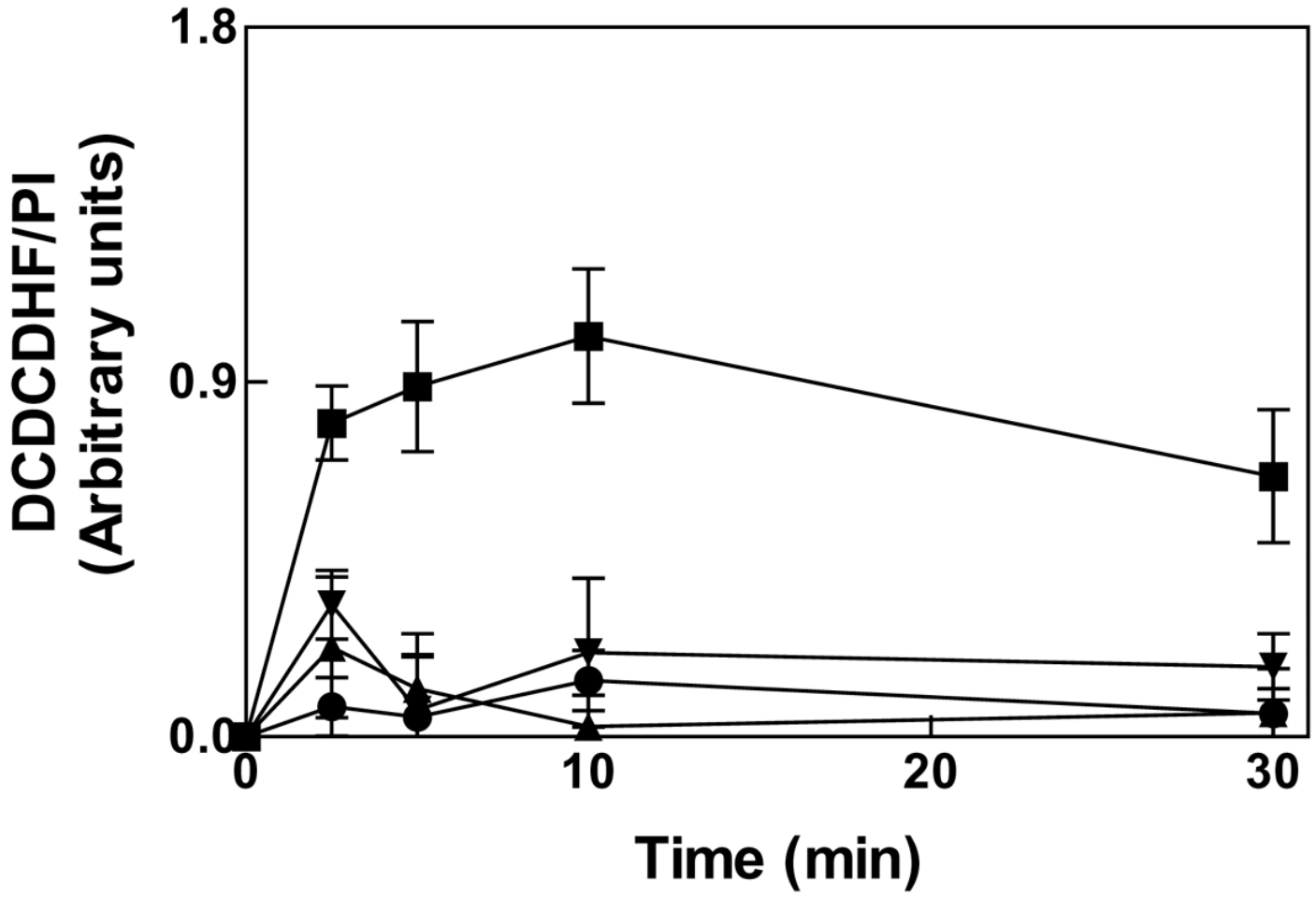

Figure 5. EC, CT, and DP-B prevent PMA increase in cell oxidants. Global oxidant levels were evaluated by DCDCDHF fluorescence in Jurkat cells after incubation with PMA alone (■) or in cells pretreated with 8.6 μM EC (▲),17.2 μM CT (▼), or 17.2 μM DP-B (●) for 24 h and a further incubation with 100 ng/ml PMA for 2.5–30 min. Global oxidant levels were determined as described in Materials and Methods. DCDCDHF fluorescence was normalized to the propidium iodide (PI) fluorescence. Results are shown as means ± SE of five independent experiments

Fig. 6

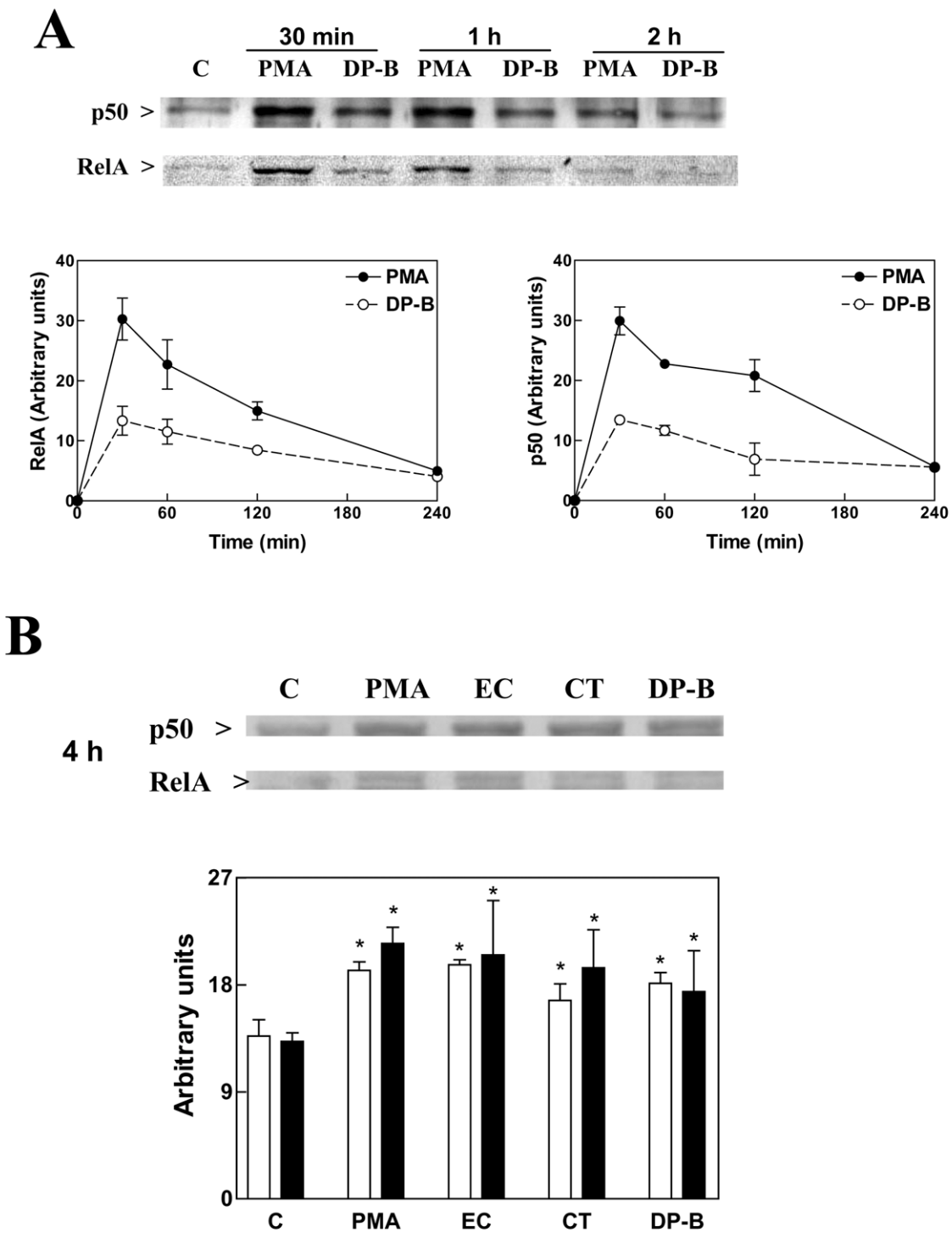

Figure 6. Evaluation of the nuclear concentration of NF-κB proteins measured by Western blot. Nuclear fractions were isolated as described in Materials and Methods. ***A)*** Kinetics of Western blot for p50 and RelA concentrations in nuclear fractions isolated from cells incubated for 24 h in media without (●) or with (○) 17.2 μM DP-B and further incubated with 100 ng/ml PMA (PMA, control cells incubated with PMA). ***B)*** Western blot for RelA and p50 in nuclear fractions after 24 h of preincubation in the absence (control, C) or presence of 8.6 μM EC, 17.2 μM CT, or 17.2 μM DP-B and further incubated without (C) or with (PMA [control cells incubated with PMA], EC, CT, DP-B) 100 ng/ml PMA for 4 h. After quantitation of Western blots, results for RelA (empty bars) and p50 (full bars) are shown as means ± SE of five independent experiments. *Significantly different compared with C (P<0.01, one-way ANOVA).

Fig. 7

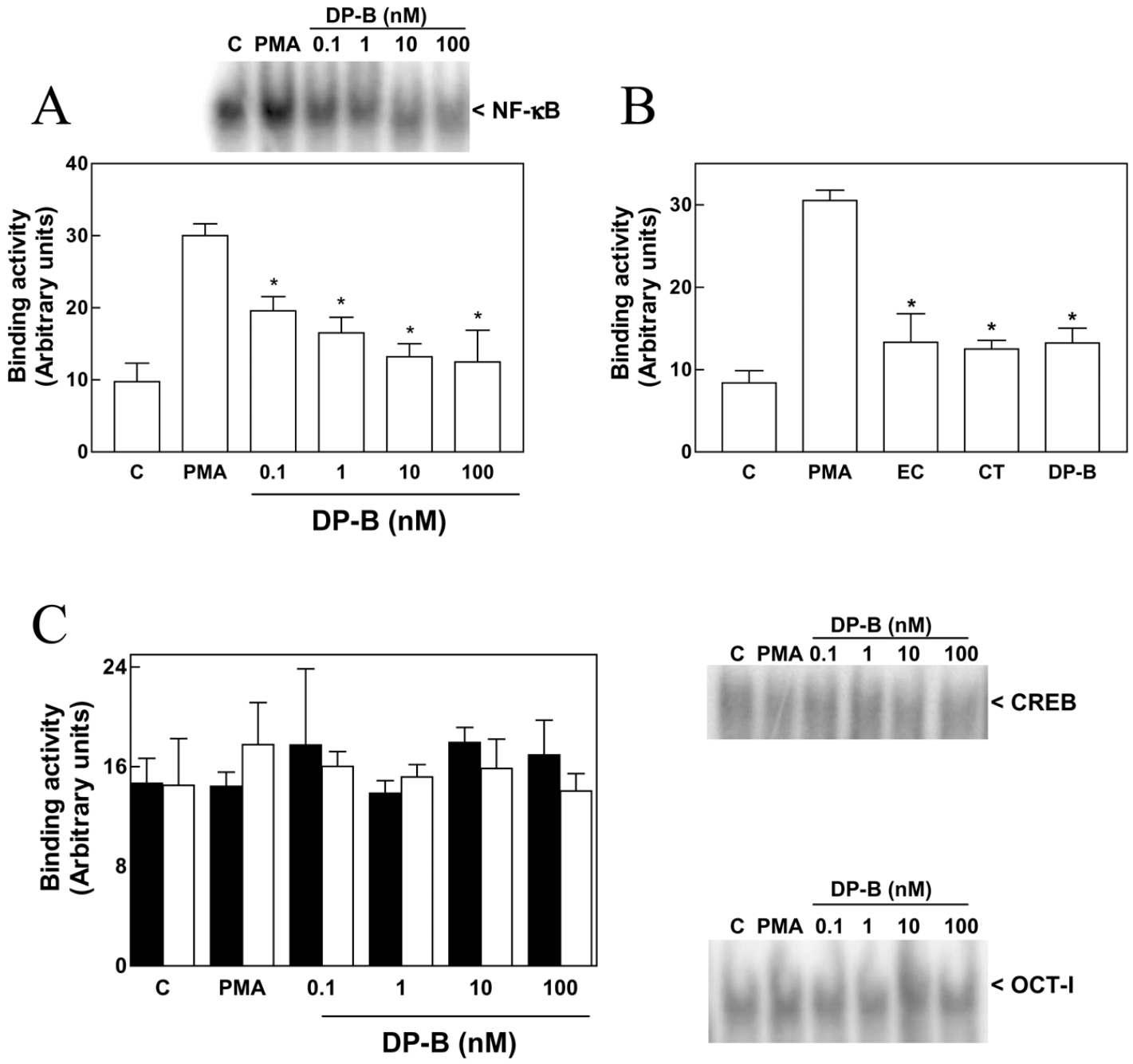

Figure 7. EC, CT, and DP-B prevent in vitro NF-κB, but neither CREB nor OCT-1 binding to DNA. NF-κB binding activity was measured by EMSA in nuclear fractions isolated from cells incubated for 4 h with 100 ng/ml PMA. Nuclear fractions were incubated with 0.2–200 nM EC, 0.2–200 nM CT, or 0.1–100 nM DP-B for 30 min before the EMSA assay. NF-κB binding activity of nuclear fractions incubated with 0.1–100 nM DP-B (***A***) or 20 nM EC, 20 nM CT, or 10 nM DP-B (***B***). ***C)*** Nuclear fraction samples from PMA-treated cells were incubated with 0.1–100 nM DP-B for 30 min before the binding assay for CREB (full bars) or OCT-1 (empty bars). After quantitation, results are shown as means ± SE of five independent experiments. *Significantly different compared with the PMA group (P<0.01, one-way ANOVA).

Fig. 8

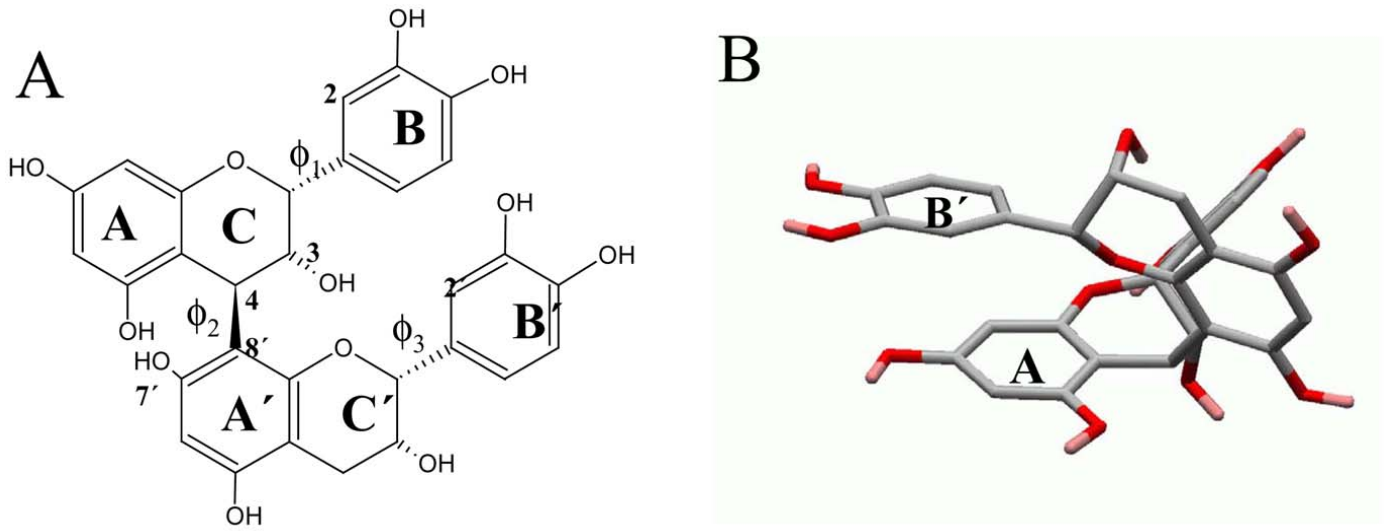

Figure 8. Structure of DP-B. ***A)*** Planar representation showing ring nomenclature and torsion angles (ϕ) critical for determining the conformation. The definition of dihedral angles follows the convention: ϕ_1, C_2-C-C-O; ϕ_2, C_3-C_4-$C_{8'}$ -$C_{7'}$; and ϕ_3, $C_{2'}$-C-C-O. The global energy minimum structure shows the following values for these angles: ϕ_1, –36.6; ϕ_2, –79.8; and ϕ_3, 134.2. ***B)*** Polytube conformational representation of the global minimum energy conformer of DP-B found after the optimized Monte Carlo search, as implemented in MacroModel (see Materials and Methods). Carbon atoms are represented in gray, oxygen atoms in red, and hydrogen atoms in pink.

Fig. 9

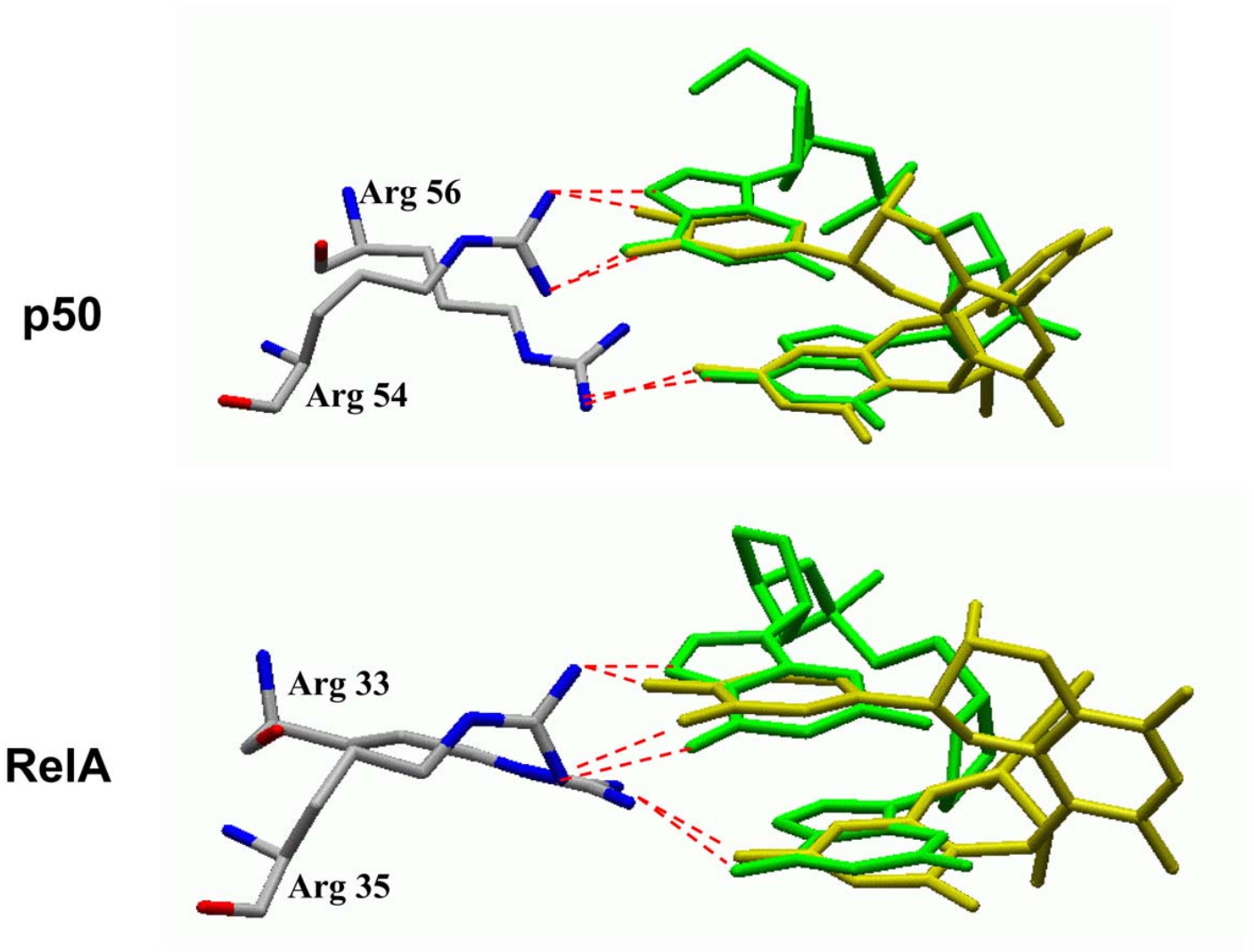

Figure 9. Superimposition between DP-B and guanine pairs. Superimposition of the minimum energy conformer of DP-B (in yellow) upon the guanine pairs (in green) taken from the double dodecamer in the complex 1VKX (35). Putative hydrogen bonding interactions (in red) mediated by Arg residues of p50 subunit (top) or RelA subunit (bottom) are shown.

Fig. 10

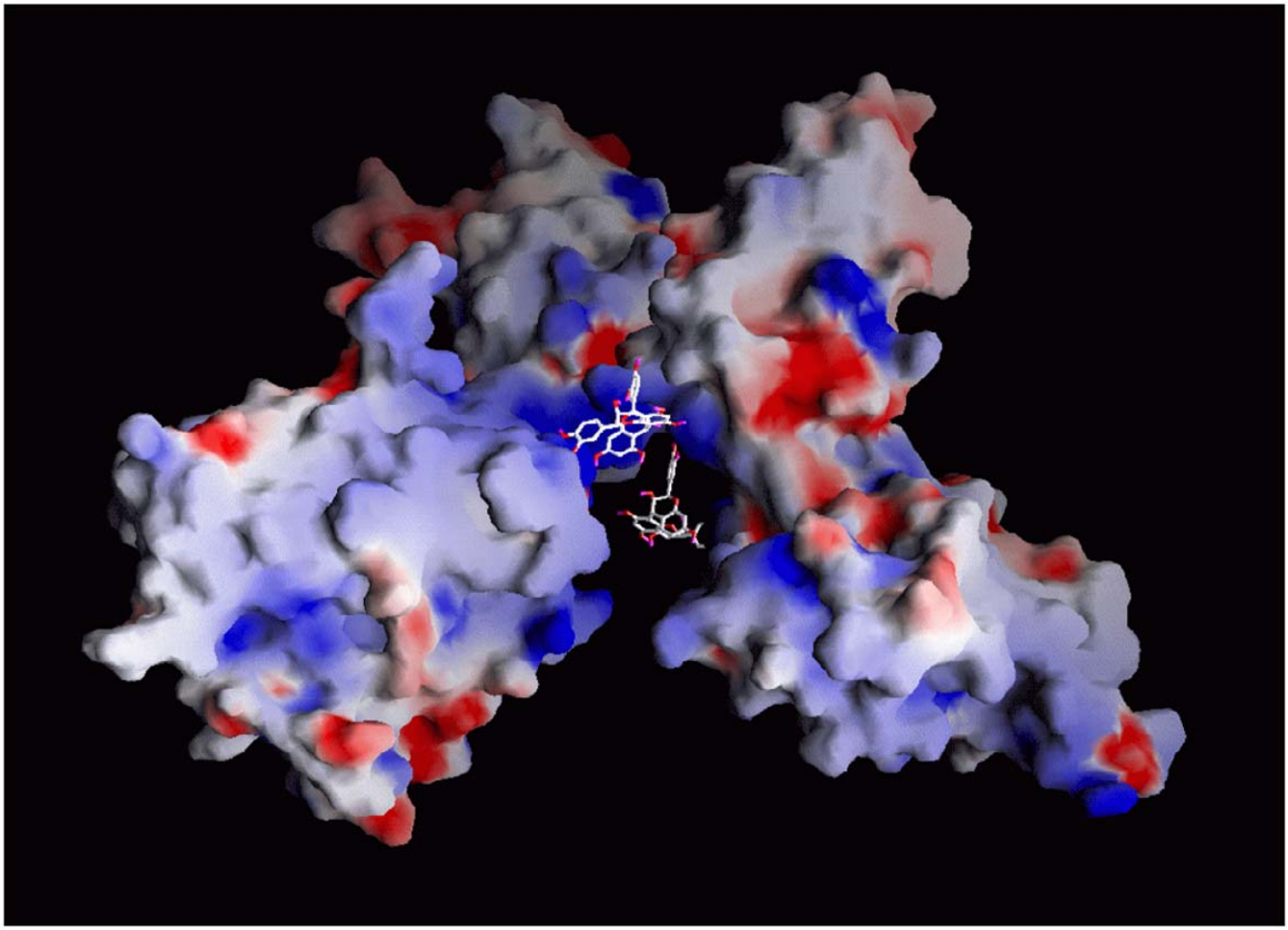

Figure 10. Representation of DP-B bound to NF-κB. Molecular area colored by the electrostatic surface potential of NF-κB (PDB entry 1VKX) is shown, as calculated by GRASP (54). Fully saturated red and blue correspond to approximately –10 k_BT/q and +10 k_BT/q, respectively. Two DP-B molecules are positioned in place of the two guanine pairs present in the κB-DNA recognition sequence: one interacting with Arg 54 and Arg 56 of p50, and the other with Arg 33 and Arg 35 of RelA.